Received: 9 June 2019 | Accepted: 20 June 2019

DOI: 10.1002/pamm.201900500

Computational Modelling of Inertia Friction Welding

Ross Williams[1,*], **Daniele Barbera**[1], **Mark Docherty**[1], **Simon Bray**[2], and **Andrew McBride**[1]

[1] University of Glasgow, School of Engineering, University Avenue, G12 8QQ, Glasgow, UK
[2] Rolls-Royce plc, PO Box 31, Derby, DE24 8BJ, United Kingdom

This study details the development and validation of a finite element methodology to robustly simulate the inertia friction welding (IFW) process. There are many difficulties involved in modelling IFW. These include the short and violent process to complete a weld, as well as the challenges in obtaining experimental data throughout the process to complement, validate and inform the modelling effort. The objectives here are to model the macroscale multiphysical process leading to an accurate prediction of key process output variables, ultimately leading to a reliable method for predicting the post weld microstructure.

© 2019 The Authors *Proceedings in Applied Mathematics & Mechanics* published by Wiley-VCH Verlag GmbH & Co. KGaA Weinheim

1 Introduction

In several industries, the joining of complex alloys and dissimilar materials is not possible using conventional fusion welding processes and requires specialised techniques. An example is the use of nickel superalloys in aerospace applications. Inertia friction welding (IFW) is a particular class of solid state welding technique, which has been intensely investigated [1–4]. The process is driven by the frictional contact at the weldline whereby the temperature of the material is raised during the initial conditioning phase in order to promote plastic flow. The large amount of energy transferred from the flywheel to the localised weld interface induces steep thermal gradients. However, the resulting heat affected zone (HAZ) is smaller than those obtained by traditional techniques. IFW-joined workpieces can be divided into four regions: the weldline which was the weld interface before the workpieces were joined, the thermo-mechanically affected zone (TMAZ) where the high temperatures and plastic deformations can result in microstructural changes, the HAZ where there is no plasticity, and the parent material which remains unchanged by the process.

1.1 The finite element model

The domain is discretised using axisymmetric elements, with an additional out-of-plane twist component. The nodes of the top workpiece (the spindle side) are linked to the flywheel master node via a relation that couples the axial displacement and the rotational speed. The nodes on the bottom workpiece (fixture side) are fully fixed. The main load acting is the normal pressure applied on the top of the model.

Two possible contact scenarios are considered: self-contact between the flash and the main part, and contact at the weld line. The former is modelled considering only normal contact behaviour. This is because when the flash comes into contact with the workpiece, the rotational speed is the same (since they are the same body). The weld line contact is modelled considering both normal and tangential behaviour. The tangential behaviour is numerically implemented via a user Fortran subroutine using the shear layer approach, which considers the material yield stress in shear which is, in turn, a function of temperature. The thermal BCs, implemented through the use of a user-defined flux subroutine with an initial workpiece temperature of 20°C. It should be noted that although radiation is considered on both the fixture and spindle, forced convection is accounted for only on the spindle side, whilst natural convection relations are implemented on the fixture. There is no thermal contact between the workpieces. A 4-noded, thermally-coupled, hybrid, reduced integration, twist element is used. This type of element accommodates the near-incompressible response of the material when it undergoes finite plastic deformations.

Importantly, a Johnson-Cook (J-C) type, isotropic, von Mises flow rule is used here. Tabulated experimental data has been used by previous researchers. The use of this constitutive model allows for the smooth evolution of the yield surface even when high-temperature experimental data may be noisy and hard to obtain. Whilst more complex models exist for predicting the yield stress of nickel superalloys [5], the simple phenomenological law proposed here is based on the three commonly used state variables in classical rate-dependent thermoelastoplasticity; strain, strain rate and temperature. In addition, nickel superalloys are strengthened by the presence of a precipitated γ' phase [6]. This phase is seen to dissolve at the weld line in IFW, where the highest temperatures are experienced [7]. As such, it is important to account for this behaviour in the modified Johnson-Cook (MJC) model. When using the Hencky model, this allows finite strain plasticity problems to be solved in a manner similar to that of the small-strain problem. The MJC model implemented is of the form

$$\sigma_y = \left[A + B\bar{\varepsilon}^{\mathrm{p}\,n}\right]\left[1 + C(\dot{\varepsilon}^*)\ln\dot{\varepsilon}^*\right]\left[1 - D(\dot{\varepsilon}^*, T^*)T^{*\,m(T^*)}\right]G(T^* \tag{1}$$

This takes a similar form to the standard J-C model, with a Ludwik hardening response characterising the isothermal, rate-independent inelastic response scaled for different temperatures and strain rates. For the rate and temperature dependence,

* Corresponding author: e-mail r.williams.2@research.gla.ac.uk, phone +44 141 330 1712

This is an open access article under the terms of the Creative Commons Attribution License 4.0, which permits use, distribution and reproduction in any medium, provided the original work is properly cited.

modifications have been made to represent the behaviour over the wide operating range. Firstly, both the strain rate sensitivity and thermal softening parameters have been converted into functions of their respective state variables, i.e., $C(\dot{\varepsilon}^*)$ and $m(T^*)$. Secondly, additional functions, $D(\dot{\varepsilon}^*, T^*)$ and $G(T^*)$, have been included. $D(\dot{\varepsilon}^*, T^*)$ has been added to account for the difference in thermal softening exhibited at different strain rates. This is seen to reduce the influence of $T^{*m(T^*)}$ on softening the material. The addition of $G(T^*)$ is essential in representing the material's actual response. The *solvus function* acts to reduce the material flow stress at temperatures where the strengthening γ' phase is expected to dissolve. This brings about a severe softening response at the macroscale and must be accounted for.

2 Results and Conclusions

In Figure 1a, the upset predicted by different material models and thermal BCs are compared with the data obtained from a weld trial. An initial discrepancy for $t \in [0, 2.0]$ is apparent and it is caused by a ramping of pressure during contact initiation in the experimental weld. This is reproduced in the numerical model by applying the pressure in two instantaneous stages. The best match to experimental data is obtained with the newly introduced MJC model and thermal BCs. If not considered, overestimation or underestimation of the final upset occurs. Thermal histories for the different scenarios are presented and compared with experimental data in Figure 1b. This data was recorded via a type N thermocouple at 1.95 mm from weldline and 2.25 mm from outer radius. The results show reasonable agreement. The embedded thermocouples have been fixed in position using high-temperature embedding cement. This contributes to additional thermal resistance at the start of the process. Also, after ∼4 s, the thermocouple was ejected when flash formation occurred, initially cooling in air before coming into contact with the hot flash, causing the abrupt overshoot. Overall, the model predicts the upset and the variation in temperature with very good precision. Due to the nature of the frictional contact algorithm used, in order for this to be predictive, the model is seen to underestimate the torque generated by the forging stage at the end of upsetting. Future work will aim to tackle this limitation, be validated against more complete thermal data and provide a comparison of the predicted mechanical fields with experimental data.

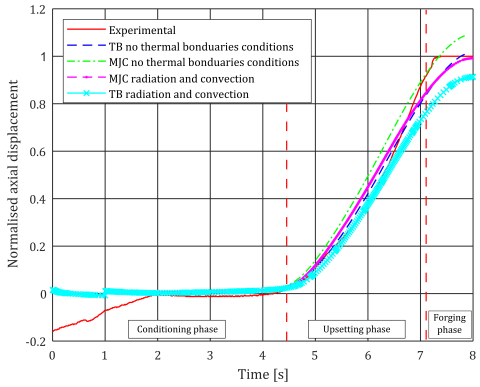

(a) Upset normalised against final experimental upset.

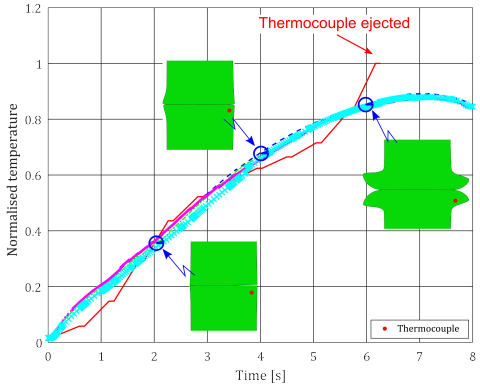

(b) Thermal profiles normalised against maximum experimental temperature.

Fig. 1: Comparison with experimental data.

Acknowledgements This research was carried out within the Materials and Manufacturing Research Group at the University of Glasgow with financial support from Rolls-Royce plc, Aerospace Group and the EPSRC NPIF. The views expressed in this paper are those of the authors and not necessarily those of Rolls-Royce plc, Aerospace Group.

References

[1] L. Fu, L. Duan, and S. Du, Welding Journal - New York **82**(3), 65–S (2003).
[2] B. Grant, M. Preuss, P. Withers, G. Baxter, and M. Rowlson, Materials Science and Engineering: A **513**, 366–375 (2009).
[3] D. Schmicker, K. Naumenko, and J. Strackeljan, Computer Methods in Applied Mechanics and Engineering **265**, 186–194 (2013).
[4] F. Wang, W. Li, J. Li, and A. Vairis, The International Journal of Advanced Manufacturing Technology **71**(9-12), 1909–1918 (2014).
[5] G. Chen, H. Qin, C. Wang, C. Yi, and P. Zhang, Metals **6**(7), 161 (2016).
[6] R. C. Reed, The Superalloys: Fundamentals and Applications (Cambridge University Press, Cambridge, 2006).
[7] M. Preuss, P. J. Withers, J. W. L. Pang, and G. J. Baxter, Metallurgical and Materials Transactions A **33**(10), 3215–3225 (2002).

© 2019 The Authors *Proceedings in Applied Mathematics & Mechanics* published by Wiley-VCH Verlag GmbH & Co. KGaA Weinheim